Chapter 6
Real-Time Hybrid Substructuring Using an Inertial Shaker Transfer System

David Vanasse III, Sergio Lobo-Aguilar, and Richard Christenson

Abstract Real-time hybrid substructuring (RTHS) is proposed as a cyber-physical method, combining both experimental and numerical testing, to capture the system-level dynamic interaction between numerical and physical substructures. With RTHS, a structural dynamic system can be partitioned into separate experimental and numerical components or substructures and interfaced together as a cyber-physical system similar to hardware-in-the-loop (HWIL) testing. The substructures that are well understood are simulated in real time using analytical or numerical models, while the substructures of particular interest, overly complex, or nonlinear are tested experimentally using physical specimens. In an RTHS test, the experimental and numerical substructures communicate together in real time by transferring displacement and force signals through a feedback loop using controlled actuation and sensing.

In a typical RTHS configuration, a transfer system is used to impart numerically determined displacements onto the physical substructure, and force sensors are used to measure the resulting restoring forces. The measurements are feed back into the numerical model to determine the displacement response at the next integration time step. Depending on the structural system's configuration, this traditional RTHS substructuring approach may not be desirable, and it may be required to apply forces or loads to the physical substructure through the transfer system and measure the specimen response (displacement or acceleration) for input to the numerical component. This might be the case for fluid–structure interaction problems or for physical testing of the bottom floor of a multistory building – as proposed here with use of an inertial shaker as the transfer system. In this study, an inertial shaker is utilized to transfer story shear force from the numerical substructure to the physical substructure.

Keywords Real-time hybrid substructuring · Inertial shaker

6.1 Introduction

This research will first demonstrate the successful completion of a real-time hybrid substructuring (RTHS) test in a traditional manner, then make an extension to a newly proposed method using an inertial shaker to apply force feedback. For RTHS tests with force feedback, there is certainly concern for closed-loop system stability [1–5]. Typical applications of RTHS with force applied by the transfer system utilize a hydraulic actuator attached between an inertial frame of reference and the substructure interface on the physical component [1]. The system being examined here is a two-story seismically excited building model, first investigated with the bottom story numerically modeled and top story physically tested. The closed-loop system will be shown to capture the dynamic interaction between the two stories and provide realistic system-level seismic response of the building system. The setup and procedure for physically testing the bottom story while numerically modeling the top story is then proposed. For this novel approach, the first story is subjected to a ground acceleration as it sits upon a bench-scale shake table and the calculated story shear [1] of the top floor is imparted to the top of the first story through the use of an inertial shaker as the transfer system. In turn, the absolute acceleration of the top of the first story is measured

D. Vanasse III
Department of Mechanical Engineering, University of Connecticut, Storrs, CT, USA

S. Lobo-Aguilar
Department of Civil Engineering, University of Costa Rica, San Jose, Costa Rica

R. Christenson (✉)
Department of Civil and Environmental Engineering, University of Connecticut, Storrs, CT, USA
e-mail: rchriste@engr.uconn.edu

M. Allen et al. (eds.), *Dynamic Substructures, Volume 4*, Conference Proceedings of the Society for Experimental Mechanics Series, https://doi.org/10.1007/978-3-031-36694-9_6

with an accelerometer and used as input to a numerical model of the top story of the building structure. The dynamics and procedure of the inertial shaker approach will be well defined to lay framework for future research on more advanced RTHS testing.

As RTHS continues to become more feasible due to advances in numerical computing power, digital signal processing, and high-speed actuation [6–8], innovation in the general framework and coupling of the substructures should be further explored. This research intends to promote that dialog in the substructuring community.

The structure of this chapter is as follows: Sect. 6.2 introduces the framework for this RTHS test in the two different substructuring realizations. In Sect. 6.3, the experimental setup and compensation methods are presented. The results of the testing for the traditional realization and extension to the new method are provided in Sect. 6.4. Section 6.5 is a conclusion of this research, followed by acknowledgments.

6.2 Real-Time Hybrid Substructuring (RTHS) Realizations

This section provides the conceptual substructuring of the two variations of performing an RTHS test on a two-story structure, including the interactions between the numerical and physical models. The goal of both methods is to accurately capture the full-system response to seismic excitation, without experimentally testing the full structure. This text takes a controls-based approach at RTHS as demonstrated in Fig. 6.1. Here, the numerical substructure is a linear model with measurements from the physical component as inputs, and with outputs applied to the physical substructure to close the feedback loop.

6.2.1 Realization 1

The first setup, denoted as Realization 1 herein, requires physical testing of the top story and numerically modeling the bottom story. From the physical test, the top story absolute acceleration $\ddot{x}_2^a$ is measured. The story shear V_s is calculated with Eq. (6.1), where m_2 is the second story mass. The story shear V_s is then input to a state-space model of the bottom story as a force acting on the top of the bottom story:

$$V_s = m_2 \ddot{x}_2^a \tag{6.1}$$

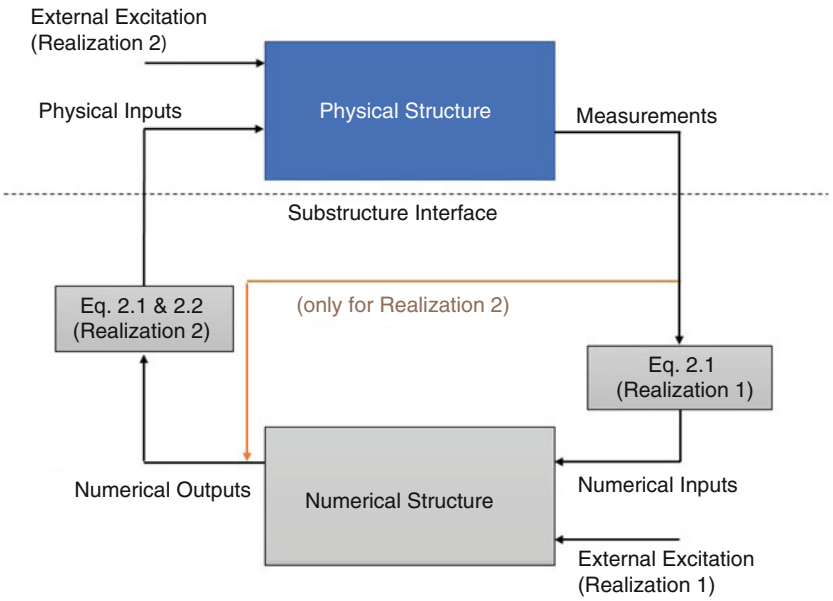

Fig. 6.1 Control-based RTHS framework

Seismic excitation of the full structure is also a numerical input. Feedback arises through application of the absolute first story displacement x_1^a as a seismic excitation at the base of the top story in the physical substructure via the shake table. The absolute first story displacement is calculated via Eq. (6.2):

$$x_1^a = x_1 + x_g \tag{6.2}$$

The value x_g is ground displacement, measured by the shake table displacement sensor for each excitation in a fully physical test. The value x_1 represents first story displacement relative to the moving base, which is computed numerically. Ground displacement is then synchronized with the measured table acceleration prior to implementation in the numerical model.

6.2.2 Realization 2

Realization 2 involves simulation of the top story, while experimentally testing the bottom story. The seismic excitation imparted by the shake table for Realization 2 is not filtered by a numerical lower story, which eliminates a potential source of error from Realization 1. However, the interaction between stories is now transferred via the inertial shaker, which is more involved due to its operation from a noninertial reference. The inertial shaker force on the first story must be equal to the story shear force that occurs at the top of floor one in the full-scale experiment. As seen by Eqs. (6.1) and (6.3), the numerical substructure requires accurate parameter values of the second story mass, and inertial shaker [active mass damper (AMD)] mass, m_2, m_{AMD} respectively to apply a force of the correct magnitude.

$$\ddot{x}_{\mathrm{AMD}} = \frac{V_s}{m_{\mathrm{AMD}}} - \ddot{x}_1^a \tag{6.3}$$

Here, $\ddot{x}_1^a$, $\ddot{x}_{\mathrm{AMD}}$, and m_{AMD} are the absolute first story acceleration, inertial shaker acceleration relative to the moving story, and inertial shaker mass, respectively. Additionally, the measurement of first story acceleration $\ddot{x}_1^a$ must have the correct magnitude with minimal delay to avoid inaccuracy and instability. Another challenge is applying the story shear from a moving reference though the inertial shaker. The inertial shaker acceleration, $\ddot{x}_{\mathrm{AMD}}$, must track the command from the numerical model in magnitude and phase. The requirements on measurement of $\ddot{x}_1^a$ and tracking of $\ddot{x}_{\mathrm{AMD}}$ are to prevent instability in the closed loop. The proposed method is more challenging due to the inertial shaker operation in a noninertial reference frame versus the traditional approach of applying story shear V_s via a hydraulic actuator from a fixed reference. However, this approach is worth investigating for extension to other systems where imparting force to the physical structure via the transfer system is of particular interest, such as fluid-loaded structures. Figure 6.2 shows the interactions between the substructures for both realizations.

6.3 Experimental Setup

This section describes the methods for each test, followed by compensation techniques. The investigated system is a reduced-scale model of a low-rise building subject to earthquake excitation. For this RTHS test, where the scaled full-system experimental test does not involve high-power consumption, is not likely to damage equipment, does not present any issues of structure size (full-scale or high-rise structure), etc., the scaled two-story physical experiment is viable for the full structure. While this is not always the case in applications when RTHS is desirable, testing the full system physically provides baseline results to evaluate the validity of the methods. In all tests, the top and bottom floor experimentally and numerically have the inertial shaker present for uniformity. In experimental tests where the inertial shaker does not play an active role, its motion is prevented by constraining its position to the end of the track. The research was performed at the National Laboratory of Structural Models and Materials at the University of Costa Rica (LanammeUCR) in San Jose, Costa Rica.

Due to the presence of feedback, actuators and sensors must be compensated to preserve stability and performance. The results are highly dependent on the tracking performance of actuators and time delay of sensors. This research implements inverse feedforward compensators designed by pole-zero placement. Section 6.3.2 shows the design process.

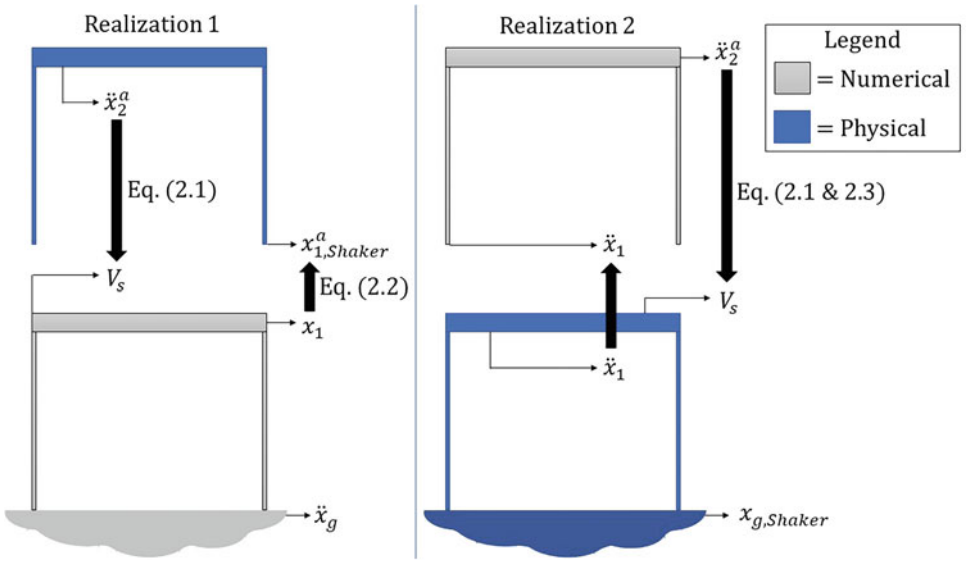

Fig. 6.2 RTHS realization diagrams

Fig. 6.3 Full structure setup

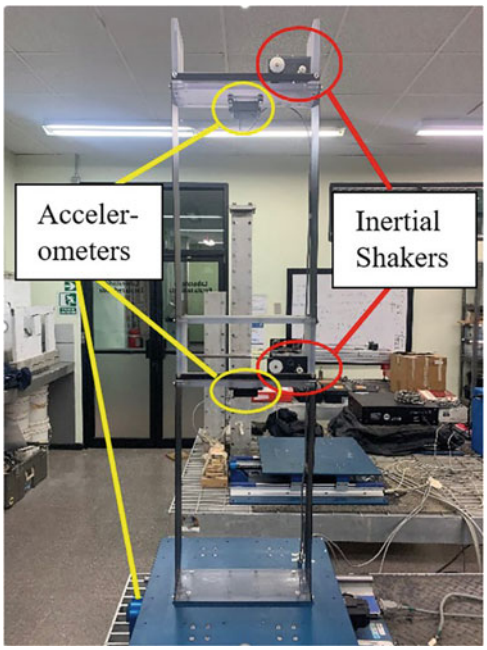

6.3.1 Fully Experimental Setup

The two-story physical structure shown in Fig. 6.3 consists of two stacked single-story sections. Each single story is constructed by mounting a Quanser AMD-2 cart with a Faulhaber Coreless DC Motor 2338S006 atop a Quanser AMD-2 structure. The inertial shakers (AMD-2 carts) use a Quanser VoltPAQ-X2 2 Channel Linear Voltage Amplifier. In the full structure test, both inertial shakers are locked in place, so they do not translate relative to the story. The structure is secured to a Quanser Shake Table II providing seismic excitation at the base of the first story. Sensors include Quanser capacitive DC accelerometers with full-scale range $\pm$ 5g, mounted to the shake table and each story of the structure. The shake table has a built-in displacement sensor. The actuators include the Quanser shake table and the two inertial shakers that remain inactive for this experiment. MATLAB/Simulink with QuaRC for Windows – Real-Time Control Software is the DAQ interface as well as control module. The Quanser Shake Table II and amplifier are powered with a Quanser UPM180-25PWM-B Universal Power Module (180 V, 25 A) – PWM-B.

To perform system identification, a band-limited white noise (BLWN) is first applied as seismic excitation to the two-story structure. The measured ground and story acceleration time histories are used to find frequency response functions (FRFs) from input (ground acceleration) to output (floor acceleration). The test structure is modeled as a two-degree-of-freedom structure with modal damping as outlined in [9]. From the measured FRF, natural frequencies and modal damping are experimentally determined.

Next, the full physical structure is subjected to various seismic excitations including both near-field and far-field earthquakes. These measurements will be used to evaluate the RTHS test performance.

6.3.2 *Fully Numerical Setup*

A numerical model of the full structure is generated as a foundation for the numerical substructures in the RTHS tests. The accuracy of the numerical model in each realization is crucial to avoid instability or inaccurate results. Equation (6.4) governs the motion for the two-degree-of-freedom lumped parameter model, adopted as a slight variation of the model used extensively for seismic vibration mitigation via MR dampers [8, 10–12].

$$\mathbf{M}\ddot{\mathbf{x}} + \mathbf{C}\dot{\mathbf{x}} + \mathbf{K}\mathbf{x} = -\mathbf{M}\boldsymbol{\Lambda}\ddot{x}_{\mathrm{g}} \tag{6.4}$$

The system matrices are.

$\mathbf{M} = \begin{bmatrix} m_1 & 0 \\ 0 & m_2 \end{bmatrix}$	$\mathbf{C} = \begin{bmatrix} c_1 + c_2 & -c_2 \\ -c_2 & c_2 \end{bmatrix}$
$\mathbf{K} = \begin{bmatrix} k_1 + k_2 & -k_2 \\ -k_2 & k_2 \end{bmatrix}$	$\boldsymbol{\Lambda} = \begin{bmatrix} -1 \\ -1 \end{bmatrix}$

Matrices **M**, **C**, and **K** are the mass, damping, and stiffness matrices, respectively, while **Λ** is a location vector as defined above. The parameters m_i, c_i, k_i are the lumped story mass, lumped flexural element damping, and lumped flexural element stiffness, respectively, for the *i*th floor. Stiffness values are determined by evaluating the steel columns as fixed-fixed beams, and modal damping is applied to determine the viscous damping coefficients. By Eq. (6.4), the continuous system has been simplified to a two-degree-of-freedom model and the vector $\mathbf{x} = [x_1\ x_2]^{\mathrm{T}}$ consists of the displacement of the bottom and top stories relative to the moving base, respectively. The command to the Quanser shake table is a displacement time history; however, the table accelerometer provides measurement of ground acceleration $\ddot{x}_{\mathrm{g}}$ to be stored for numerical application. The higher-order nonlinear effects do not significantly impede the numerical model from matching the experimental data. Equation (6.4) can be written in state-space form of Eqs. (6.5) and (6.6) by defining the state vector $\mathbf{z} = [\mathbf{x}\ \dot{\mathbf{x}}]^{\mathrm{T}}$, input scalar as $u = \ddot{x}_{\mathrm{g}}$, which is recorded prior from fully physical tests, measurement vector $\mathbf{y} = \left[\ddot{x}_1^a\ \ \ddot{x}_2^a\ \right]^{\mathrm{T}}$, and matrices A–D accordingly. For the story accelerations within the measurement vector, subscripts 1 and 2 represent first and second story, respectively, while superscripts "a" indicate an absolute measurement:

$$\dot{\mathbf{z}} = \mathbf{A}\mathbf{z} + \mathbf{B}u \tag{6.5}$$

$$\mathbf{y} = \mathbf{C}\mathbf{z} + \mathbf{D}u \tag{6.6}$$

$\mathbf{A} = \begin{bmatrix} \mathbf{0} & \mathbf{I} \\ -\mathbf{M}^{-1}\mathbf{K} & -\mathbf{M}^{-1}\mathbf{C} \end{bmatrix}$	$\mathbf{B} = \begin{bmatrix} \mathbf{0} \\ \boldsymbol{\Lambda} \end{bmatrix}$
$\mathbf{C} = [-\mathbf{M}^{-1}\mathbf{K}\ \ -\mathbf{M}^{-1}\mathbf{C}]$	$\mathbf{D} = \begin{bmatrix} 0 \\ 0 \end{bmatrix}$

6.3.3 Transfer System Compensation

In both RTHS methods, the stability and accuracy of the closed-loop test are heavily dependent on the sensors and actuators. In an RTHS test, both random error (sensor noise) and systematic error (actuator/sensor magnitude and phase disagreements) can be detrimental [8], though reduction of systematic error tends to be more important [13, 14]. An uncalibrated actuator will prevent displacement compatibility of the numerical model with the physical model; when actuators have a considerable time delay, or phase lag, this means the actuation happens slightly later than when it is commanded. The effect may be frequency dependent and is a common source of instability in RTHS tests [15]. Tracking of actuator excitation magnitude is also critical. This is more self-explanatory; the actuators should excite the structure at the commanded magnitude. Sensors have the same restrictions; if there is a phase lead/lag or high gain factor at frequencies of importance, the physical sensors will incorrectly feed data back into the numerical model. In this experiment, the first and second natural frequencies of the structure were experimentally determined to be 1.32 Hz and 3.58 Hz, respectively. The target frequency range of compensation for both actuators and sensors is thus 0–10 Hz.

Frequency response functions provide a convenient method for identifying the magnitude of input/measurement amplification and phase lead or lag. An FRF can be used to generate two plots: the first is the amplification in decibels versus frequency, and the second is the phase lead or lag versus frequency in degrees [16]. To collect FRFs for the shake table and inertial shaker, a band-limited white noise (BLWN) is individually commanded to each with no command sent to the other. The constant autospectral density function of a BLWN removes input bias from the FRF to accurately capture hardware dynamics [16].

To maintain fidelity of the substructuring, inverse feedforward compensation is employed as needed. This begins with building a transfer function (TF) that produces an FRF matching that of each sensor or actuator, then inverting the TF, ensuring it is stable, and placing it in line with the sensor [17]. If done successfully, the FRF of the collected data from the sensor/actuator with the feedforward compensator should have near-zero dB (unity) gain and a phase of zero degrees within the frequency range of 0–10 Hz. More detailed processes for transfer system compensation in RTHS tests such as minimum-phase inverse compensation and P-type iterative learning control are presented by [7].

The Quanser shake table and inertial shaker are equipped with a built-in feedback-feedforward position controllers and are experimentally proven to track commands well. A 10 Hz low-pass filter is implemented for all signals commanded to the shaker. The accelerometers are compensated as described above.

6.3.4 Realization 1 Setup

The first RTHS test, described in Sect. 6.2.1 and shown in Fig. 6.2, is a physical test of the top floor interacting with a numerically modeled bottom floor. The physical testbed is that of Sect. 6.3.1 without one structure, as shown in Fig. 6.4. The inertial is again locked in place for this test. The numerical bottom floor is seismically excited by the previously measured

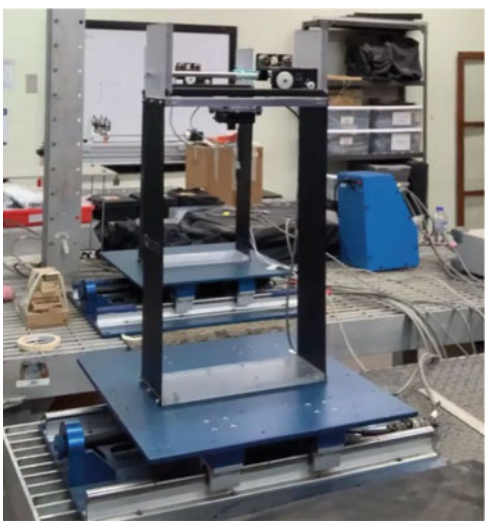

Fig. 6.4 RTHS Realization 1 experimental setup

earthquake acceleration time history, which in turn induces an acceleration to the numerical bottom floor. The only active actuator in the physical model is the shake table itself, which moves with the numerical bottom floor per Eq. (6.2). The shake table acceleration and displacement are recorded to ensure command tracking. The shake table induces motion of the physical top story, pictured in Fig. 6.4. The top story accelerometer sends a reading to the numerical model. At the next time step, this measured second story acceleration is converted to a story shear via Eq. (6.1) and input to the numerically simulated first story state-space model. The physical/numerical interface crossings can be realized by the numerical first story absolute displacement sent to the shake table command, and conversely the physical second story acceleration converted to a story shear imposed on the numerical first story.

The state-space model requires modification from its form in Sect. 6.3.1 to numerically model the bottom floor only. The equations of motion for the bottom floor can be written in the form of Eqs. (6.5) and (6.6) if the state vector is replaced by $\boldsymbol{z_1} = [x_1 \dot{x}_1]^{\mathrm{T}}$, input scalar is replaced by input vector $\mathbf{u_1} = \left[\ddot{x}_{\mathrm{g}} \;\; V_{\mathrm{s}}\right]^{\mathrm{T}}$, output vector is replaced by $y_1 = \left[x_1 \ddot{x}_1^a\right]$, and matrices **A–D** are rewritten as a new $\mathbf{A_1}$-$\mathbf{D_1}$ as follows:

$$\mathbf{A_1} = \begin{bmatrix} 0 & 1 \\ \frac{-k_1}{m_1} & \frac{-c_1}{m_1} \end{bmatrix} \qquad \mathbf{B_1} = \begin{bmatrix} 0 & 0 \\ -1 & \frac{1}{m_1} \end{bmatrix}$$

$$\mathbf{C_1} = \begin{bmatrix} 1 & 0 \\ \frac{-k_1}{m_1} & \frac{-c_1}{m_1} \end{bmatrix} \qquad \mathbf{D_1} = \begin{bmatrix} 0 & 0 \\ 0 & \frac{1}{m_1} \end{bmatrix}$$

Here, the states and outputs are all for the bottom floor, as indicated by the subscript.

6.3.5 *Realization 2 Setup*

The second RTHS test proposed by this research is a simultaneous numerical simulation of the top story and experimental test of the bottom story in real time. The physical testbed is identical to Fig. 6.1; however, the inertial shaker is no longer locked in place. Any mass above the bottom story moving along with x_1 is considered negligible. The sensors required include accelerometers on the inertial shaker, physical top floor, and shake table. Actuators in this method include the shake table and inertial shaker.

This nontraditional setup is more involved than that of Sect. 6.3.3. The ground motion is directly applied by the shake table physically, and the subsequent first story displacement is feed into the numerical model. The first story measured acceleration seismically excites the simulated top floor. The numerical top floor acceleration is then converted to a story shear via Eq. (6.1). Next, the measured bottom floor acceleration $\ddot{x}_1^a$ and calculated story shear V_{s} are input to Eq. (6.3) to determine the inertial shaker acceleration $\ddot{x}_{\mathrm{AMD}}$ required to produce that same shear force. The commanded displacement x_{AMD} is relative to the moving first story and is required to command the AMD. The measurement $\ddot{x}_1^a$ is necessary because the inertial shaker acts in a noninertial reference frame. To avoid damage, $\ddot{x}_{\mathrm{AMD}}$ is integrated twice to determine x_{AMD}, which is compared to the allowable stroke.

Again, a new state-space model must be developed with a new state vector $\boldsymbol{z_2} = [x_2 \dot{x}_2]^{\mathrm{T}}$, new input defined as scalar $u = \ddot{x}_1^a$, new output defined as scalar $y_2 = \ddot{x}_2^a$, and matrices **A–D** are rewritten as a new $\mathbf{A_2}$-$\mathbf{D_2}$ as follows:

$$\mathbf{A_2} = \begin{bmatrix} 0 & 1 \\ \frac{-k_2}{m_2} & \frac{-c_2}{m_2} \end{bmatrix} \qquad \mathbf{B_2} = \begin{bmatrix} 0 \\ -1 \end{bmatrix}$$

$$\mathbf{C_2} = \begin{bmatrix} \frac{-k_2}{m_2} & \frac{-c_2}{m_2} \end{bmatrix} \qquad \mathbf{D_2} = \begin{bmatrix} 0 \end{bmatrix}$$

With the interactions across the physical/numerical interface modeled correctly, this RTHS test will be successful with sensors and actuators that track sufficiently well.

6.4 Results

The goal of this study is to validate traditional RTHS proceedings and present a new approach via realizations 1 and 2, respectively. Realization 2 can be extended to a variety of complex tests to reduce the degree of complication. RTHS testing additionally reduces the scale of failures due to the reduction in dynamic physical components.

6.4.1 System Identification

To adjust the state-space models, a BLWN is applied as seismic excitation to the full physical 2DOF structure as outlined in Sect. 6.3.1. The BLWN is a low-pass white noise with a 10 Hz cutoff frequency, chosen per the structural natural frequencies. The resulting FRFs from ground acceleration to story acceleration are shown in Fig. 6.5.

The numerical model matches the physical model in terms of dynamics, including natural frequencies and damping ratios within the frequency range of concern. This validates the simplification to a two-degree-of-freedom model for this application.

6.4.2 RTHS Tests

Upon completion of sensor and actuator compensation, the first RTHS substructuring realization can be tested. Initially a BLWN seismic excitation is employed to ensure the single degree of freedom (SDOF) physical substructure displays two modes at the frequencies of the full physical structure (2DOF). The RTHS interactions between substructures successfully create a transformation from one natural frequency at 2.47 Hz to two natural frequencies near 1.32 and 3.58 Hz as shown in Fig. 6.6.

As shown, the RTHS test results produce a similar FRF magnitude to the full physical test; however, the second mode occurs at 3.74 Hz with 30 dB attenuation rather than 3.58 Hz with 25 dB attenuation.

Subsequently, a series of earthquake time histories are input as ground excitation to the numerical bottom floor in RTHS Realization 1 tests. Results for the 1995 Kobe, Japan, 1994 Northridge, California, and 1992 Cape Mendocino earthquakes are displayed.

As shown in Fig. 6.7, the time histories from the Kobe 1995 excitation display excellent agreement with the fully physical test performed prior, particularly for the second story, which is the physical substructure. In an RTHS test, the goal is to impart well-known dynamics to an uncertain substructure physically with the same results as a full-scale test. Therefore, the

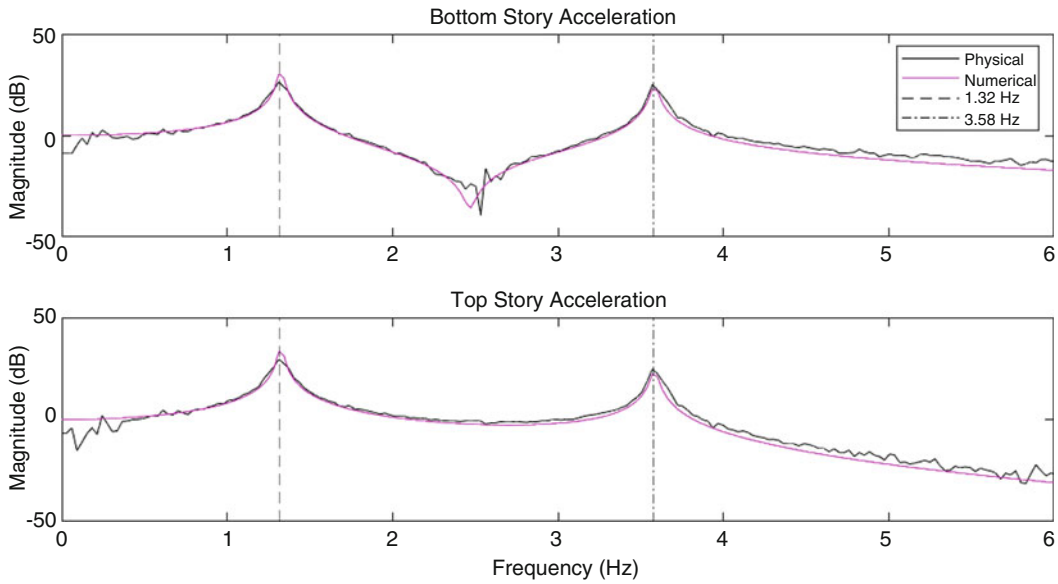

Fig. 6.5 System identification FRF magnitudes

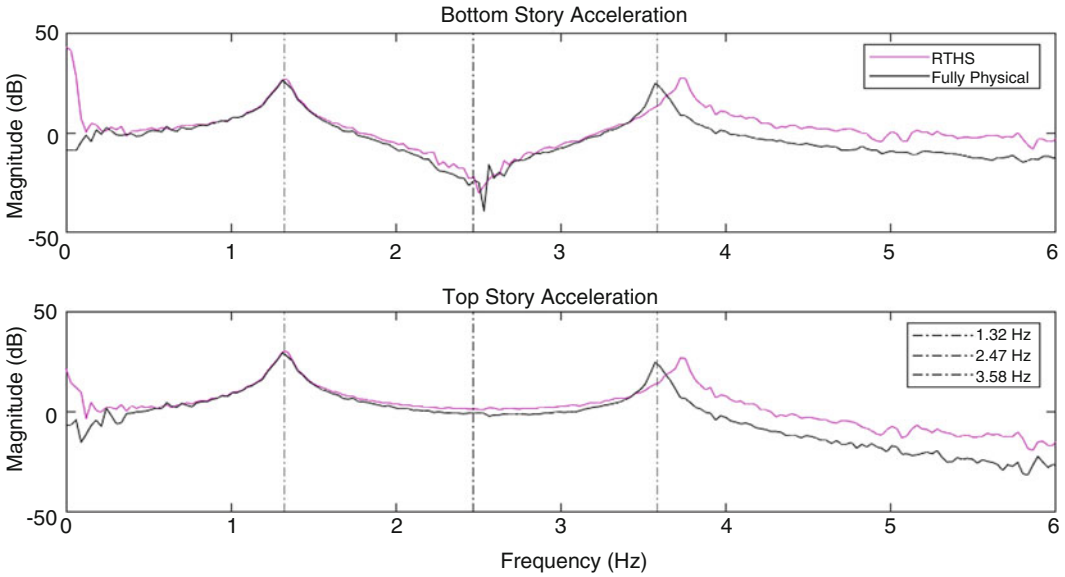

Fig. 6.6 RTHS vs. full physical FRF magnitudes

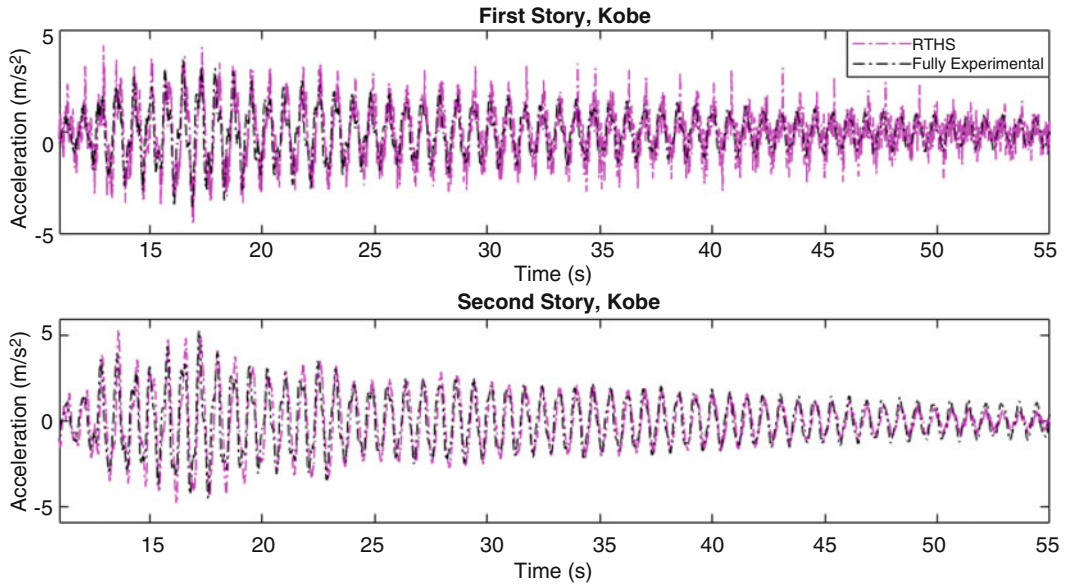

Fig. 6.7 Kobe 1995 acceleration time histories (RTHS Realization 1)

second story performance is of greater importance. Northridge and Cape Mendocino time histories exhibit better magnitude agreement for the bottom story and reduced magnitude accuracy in the second story when compared to Kobe (Fig. 6.8). All RTHS time histories are similar in nature: they underpredict first story acceleration and overpredict second story acceleration. Regardless, the frequencies and phase are in excellent agreement throughout all three tests.

Future tests will conduct RTHS Realization 2, following the procedure outlined in this chapter (Fig. 6.9).

6.5 Conclusion

This study presented the successful completion of a traditional RTHS test for a low-rise structure and proposed framework for a novel approach to investigation of the bottom floor dynamics. It has been proven that real-time hybrid substructuring provides a worthy approach to reduced-scale testing. Realization 1 has been validated by reporting closely matched FRFs

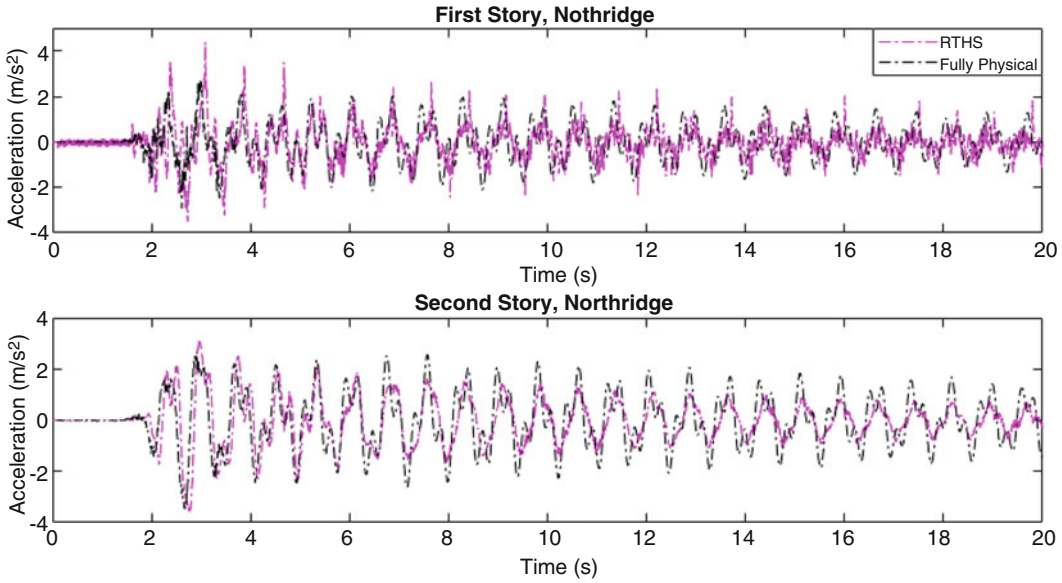

Fig. 6.8 Northridge 1995 acceleration time histories (RTHS Realization 1)

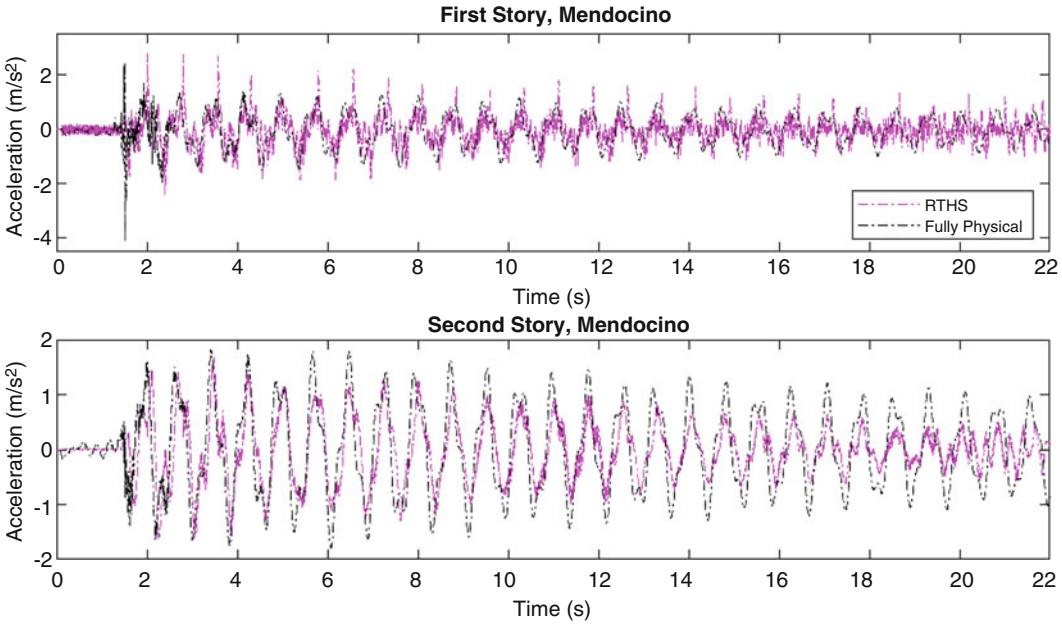

Fig. 6.9 Cape Mendocino 1992 acceleration time histories (RTHS Realization 1)

between the fully physical and RTHS tests. Furthermore, a more intuitive understanding is gained by the evidence shown in the latter portion of Sect. 6.4.2, which compares earthquake time histories between the RTHS and fully physical tests. The presence of two vibration modes in an SDOF structure further validates RTHS. The procedure for a Realization 2 setup is well defined in Sect. 6.3.3. As an extension, the numerical model for Realization 2 can be altered to represent a high-rise structure. If all interactions (story shear, seismic excitation) are transferred accurately, the method is viable. The nontraditional approach of imparting forces on the physical substructure and recording motion may be applied to a variety of complex test procedures, including wind or fluid-loaded structures.

In the Realization 1 test, the second natural frequency shown in the RTHS test attenuated more than the physical test, and it occurred at a higher value. Potentially, the system identification may have slightly overpredicted the stiffness or underpredicted mass for either structure. While both stories were the same Quanser product, one may have experienced plastic deformation due to yielding, introducing nonlinearity to the dynamics.

For future procedures conducting the Realization 2 test, it may be necessary to add a static mass to the physically tested bottom story. Justification arises through the unaccounted mass from the lower section of the top story columns that have little displacement relative to the bottom story in a fully experimental test.

Acknowledgments The authors thank the Academic Visitors Program through the Office of International Affairs and External Cooperation (OAICE) at the University of Costa Rica as well as the University of Connecticut for sponsoring travel and research, and the University of Costa Rica LanammeUCR for providing equipment and access to the lab facility to conduct the experimental testing.

References

1. Reinhorn, A., Bruneau, M., Chu, S.-Y., Shao, X., Pitman, M.: Large scale real time dynamic hybrid testing technique - shake tables substructure testing. In: The First International Conference on Advances in Experimental Structural Engineering (2005)
2. Zhao, J., French, C., Shield, C., Posberg, C.: Considerations for the development of real-time dynamic testing using servo-hydraulic actuation. Earthq. Eng. Struct. Dyn. **32**(11), 1773–1794 (2003)
3. Kyrychko, Y.N., Blyuss, K.B., Gonzalez-Buelga, A., Hogan, S.J., Wagg, D.J.: Real-time dynamic substructuring in a coupled oscillator–pendulum system. Proc. R. Soc. A. **462**, 1271 (2006)
4. Horiuchi, T., Inoue, M., Konno, T.: Development of a real-time hybrid experimental system using a shaking table (proposal of experimental concept and feasibility study with rigid secondary system). JSME Int. J. Ser. C. **42**(2), 255–264 (1999)
5. Colgate, J.E., Stanley, M.C., Brown, J.M.: Issues in the haptic display of tool use. In: Proceedings 1995 IEEE/RSJ International Conference on Intelligent Robots and Systems. Human Robot Interaction and Cooperative Robots (1995)
6. Saouma, V., Sivaselvan, M.: Hybrid Simulation: Theory, Implementation and Applications. Taylor & Francis, London (2008)
7. Insam, C., Harris, M.J., Stevens, M.R., Christenson, R.E.: Real-time hybrid substructuring for shock applications considering effective actuator control. In: IMAC-XL Sociecty for Eng. Mech. Conference, Orlando (2022)
8. Christenson, R., Lin, Y.Z., Emmons, A., Bass, B.: Large-scale experimental verification of semiactive control through real-time hybrid simulation. J. Struct. Eng. **134**(4), 522–534 (2008)
9. Inman, D.J.: Engineering Vibration. Pearson Education, Inc, Upper Saddle River (2014)
10. Dyke, S.J.: Modeling and control of magnetorheological dampers for seismic response reduction. Smart Mater. Struct. **5**, 565–575 (1996)
11. Dyke, S.J., Spencer Jr., B.F., Quast, P., Sain, M.K.: The role of control-structure interaction in protective system design. J. Eng. Mech. ASCE. **121**, 322–338 (1995)
12. Dyke, S.J., Spencer Jr., B.F., Quats, P., Kaspari Jr., D.C., Sain, M.K.: Implementation of an active mass driver using acceleration feedback control. In: Microcomputers in Civil Engineering (Special Issue on Active and Hybrid Structural Control), vol. 11, pp. 305–323 (1996)
13. Shing, P.B., Mahin, S.A.: Cumulative error effects in pseudodynamic tests. Earthq. Eng. Struct. Dyn. **15**, 409–424 (1987a)
14. Shing, P.B., Mahin, S.A.: Elimination of spurious higher-mode response in pseudodynamic tests. Earthq. Eng. Struct. Dyn. **15**(425–445), 425 (1987b)
15. Huang, L., Chen, C., Guo, T., Chen, M.: Stability analysis of real-time hybrid simulation for time-varying actuator delay using the Lyapunov-Krasovskii functional approach. J. Eng. Mech. **145**(1), 1–15 (2019)
16. Bendat, J.S., Piersol, A.G.: Random Data: Analysis and Measurement Procedures. Wiley, Hoboken (2010)
17. Franco III, J.A.: Real-time hybrid substructuring for system level vibration testing of mechanical equipment. Ph.D. Dissertation, College of Eng., Univ. of Conn., Storrs (2016). [Online]